

SHOCK AND MAGNETOPAUSE BOUNDARY  
OBSERVATIONS WITH IMP-2

by

Joseph H. Binsack

Laboratory for Nuclear Science and Center for Space Research  
Massachusetts Institute of Technology  
Cambridge, Massachusetts

Short Title: Shock and Magnetopause Observations

Presented at the Summer Institute Physics of the Magnetosphere,  
Boston College, June 19-28, 1967, Chestnut Hill,  
Massachusetts.

## I. Introduction

This paper is the first of a series reporting on the M.I.T. experiments flown on recent satellites. We shall begin by reviewing the operations of the M.I.T. Faraday cup which is the basic plasma detector used by our group. We shall then turn to some specific observations made by the IMP-2 satellite. The magnetopause and bow shock will be our main topic of discussion in this paper.

### A. Review of the M.I.T. Plasma Detector

The M.I.T. plasma detector is essentially a Faraday cup which is operated in a differential energy mode. The relatively small energy range within which the detector collects particles is determined by the alternating square wave of potential imposed on the modulator grid (grid number 2 in Figure 1). Those particles with sufficient kinetic energy to overcome the potential on the grid will reach the collector. At the higher potential of the square wave fewer particles will be collected and thus there will be an alternating current at the frequency of the modulator waveform. This A.C. signal is processed by the measurement chain, and then presented to the telemetry system for transmission to the ground receiving station. The signal is proportional to the flux of particles within the energy window determined by the voltages  $V_j$  and  $V_{j+1}$ . By varying these potentials one can obtain information concerning the differential energy spectrum of the plasma particles.

The collectors on the IMP and Pioneer series of experiments were split in half by a plane perpendicular to the satellite's spin axis; the proton experiment on the OGO satellites had a triplate collector; and the electron experiment on OGO has but a single collector. Through an analysis of the relative currents detected by each of the collector segments, one can obtain information on the flow direction in a plane defined by the instrument's viewing direction and the spin axis (the meridian plane). Information concerning flow direction in the azimuthal plane is obtained by sampling at various angular segments within a rotational period.

The third grid in the detector shields the collector from the strong fields near the modulator grid. The fourth grid suppresses secondary electrons and the photoelectrons liberated from the collector when it is illuminated by the sun.

The negative 36 volt potential for this grid for IMP-1 and IMP-2 has turned out to have been an unfortunate choice. Electrons, which are free to enter the cup when the modulation potential is positive, will undergo a net displacement, transverse to the detector's outward normal, due to the bending of the electron's trajectory by the electrostatic fields near the modulator. The greater the potential on the modulator, the greater will be the transverse displacement. The amount of displacement will be accentuated by the negative voltage on the suppressor grid, especially if the electron's kinetic energy is near the suppressor's potential. We have termed this shifting of the trajectories within the detector "refractive

modulation." It is an important consideration in the magnetosheath where the majority of electrons are just slightly above the suppressor's 36 volts. The shifting of electrons onto and away from the collector constitutes an A.C. signal which usually dominates the current in the magnetosheath. We shall return to this feature later when we consider the structure of the actual data.

#### B. The IMP-2 Satellite

The IMP-2 satellite (Explorer 21) was launched on 4 October 1964. It is perhaps not as famous as its sister satellite, launched a year earlier, due to a malfunction of the third stage rocket. The reduced performance resulted in a lower apogee and a shift in the spin axis which eventually spelled death to the electrical power system. The region of space, which was explored by IMP-2 during its three main lifetimes is shown in Figure 2. The fact that apogee was very close to the bow shock for the first 40 orbits permitted many opportunities to observe the bow shock and its spatial and temporal variations.

## II M.I.T. Plasma Observations on IMP-2

### A. General

The general character of the signals observed changes markedly throughout the orbit depending on the particular region of space being explored by the satellite. As an illustration, Fig. 3 presents a summary of the signals in each of the six energy channels of the experiment.

From 0925 hours U.T. until 1450 hours IMP-2 was in the magnetosphere. Within the magnetosphere three distinct subregions are apparent: from perigee to 1100 hours when the satellite was at a geocentric distance of 5 earth radii ( $R_e$ ), the negative channel (-130 to -265 volts) was responding to the high ion densities in the plasmasphere (Binsack, 1967). From 1100 to 1230 hours the generally low isotropic response in all channels is due to the presence of high energy trapped electrons (refractively modulated in the positive channel mode). From 1230 hours ( $7.5 R_e$ ) until the encounter of the magnetopause at 1450 hours, the detector is responding to an increasing flux of low energy electrons (approximately 1 Kev or below). The exact nature of these electrons is not yet understood. They may be related to the low energy electrons observed by Vasyliunas on OGO (for a more complete discussion of these electrons see the companion paper by Vasyliunas). Our own preliminary study has showed a tendency for their occurrence to correlate with periods of weak trapped electron fluxes in the skirt region (K.A. Anderson, private communications) and also with periods when the magnetic field direction is nearly continuous across the magnetopause (D. Fairfield,

private communication). Further study of this phenomenon is in progress.

After the magnetopause crossing at 1450 hours ( $10.5 R_e$ ), the satellite entered the magnetosheath where it remained until 1715 hours. At this time it briefly entered the interplanetary region until 1740 hours ( $13 R_e$ ). While in the magnetosheath the high flux of refracted low energy electrons (about 50 eV) is clearly seen as the background signal in each channel. The peak in each channel is a little larger than the background due to the additive effect of a flowing ionic component of the plasma in the magnetosheath.

After 1925 hours ( $14 R_e$ ) the satellite was almost continually in the interplanetary medium (brief excursions of the magnetosheath past the satellite occurred before 2200, after 2400, and again before 0300 hours on 25 Oct. 1964). The interplanetary data are characterized by a strongly roll modulated signal in one or more adjacent channels. The instrument detects the high flux of particles in the energy channel associated with the wind's bulk motion and in the direction corresponding to the bulk flow. The maximum current in the 95 to 230 eV channel is more than a factor of ten above the background and the two adjacent channels also show some degree of roll modulation.

Starting at 1000 hours ( $14 R_e$ ) on 25 Oct. 1964, multiple crossings of the bow shock were observed. After a short gap in data, the magnetosheath was continuously observed until 1340 hours ( $11 R_e$ ) at which time a sharp crossing of the magnetopause

was observed. Several other sharp crossings were observed clustered around 1445 hours. A normal magnetosphere was observed until 1730 hours ( $4.5 R_e$ ) when the plasmasphere was entered as the satellite approached perigee.

This orbit illustrates quite well many of the features seen by IMP-2: the plasmasphere and its boundary the magnetopause, the fluxes of moderately energetic electrons occasionally observed in the outer magnetosphere near the inside of the magnetopause, the high flux of lower energy electrons in the magnetosheath and the slight roll modulation in this region due to the ordered flow of the ions, the multiple crossings of both the magnetopause and the bow shock, and the directive flow of plasma from the sun when the satellite is in the interplanetary region.

## B. The Boundaries of the Magnetosheath

### 1. General Behavior and Location of the Boundaries

Using a plane defined by the sun-earth and earth-satellite lines, we have plotted the spatial location of those portions of the orbit where fluxes indicative of the magnetosheath have been observed (Figure 4). There are two general observations to which we would like to call attention:

a. The boundaries are quite pliable and respond noticeably to interplanetary activity. In particular the recurrent solar activity listed in Table I compressed the boundaries resulting in their observations at geocentric distances

well within the average positions. We have reported on this compression as observed by IMP-1, IMP-2 and OGO-1 and have shown it to agree quite well with the simple balancing of plasma dynamic pressure with a magnetic dipolar pressure (Binsack and Vasylunas, 1967).

TABLE I

| <u>Day of Solar Rotation</u> | <u>Day</u> | <u>IMP-2 Orbit</u> |
|------------------------------|------------|--------------------|
| 14-15                        | 3-5 Oct.   | 1 out              |
|                              | 1 Nov.     | 20 in              |
|                              | 28-29 Nov. | 39 out             |
| 21-22                        | 11-12 Oct. | 6 in               |
|                              | 8 Nov.     | 25 both            |
| 2                            | 19 Oct.    | 11 out             |
|                              | 15 Nov.    | 30 both            |
| 9                            | 26 Oct.    | 16 out             |
|                              | 22 Nov.    | 35 in              |

b. Even during periods of relative inactivity of the interplanetary solar wind, the boundaries display a great degree of variability. There was scarcely a single orbit which was observed not to have multiple crossings of the bow shock and/or magnetopause. The detailed spatial and temporal behavior of the boundaries for the first seven orbits are illustrated in Figure 5. Note particularly that even several earth radii beyond the expected position of the bow shock, plasma is occasionally observed which is characteristic of the magnetosheath.



Geomagnetic activity was moderate ( $K_p \leq 3$ ) during orbits 2, 3, and 4, while it was relatively quiet during orbits 5 and 6. The activity was quite high ( $K_p \sim 5$ ) during Orbit 1 yet there were no observations of magnetosheath plasma beyond the expected bow shock position. Note, too, that the magnetopause also exhibits motion and structure.

It is our opinion that both boundaries are seldom, if ever, stationary surfaces, but rather exhibit motion even during periods of relatively quiet solar and geomagnetic activity.

## 2. Observations within the Boundary Layers

Let us now turn to a closer look at these boundaries by using the plasma data in all of their available detail. From the vantage point of a spinning satellite, we are able to study the plasma characteristics in angle as well as in energy. During the early life of IMP-2, the spin period was slightly longer than the data frame period (a result of the malfunction of the third stage rocket), and thus only about 80 percent of an azimuthal scan could be obtained at a constant energy channel. If we now translate the available data onto an axis from  $-180^\circ$  to  $0^\circ$  to  $+180^\circ$ , where zero degrees corresponds to the time when the detector was closest to the satellite-sun line, we obtain plots of the form illustrated in Figures 6, 7, 8, and 9. Note that the data have been folded over so that they all lie between  $-180^\circ$  and  $+180^\circ$  with the starting time of the frame occurring after the small gap in data (a factor due to the frame period being less than the spin period). The time and sequence

numbers show on the left of each figure relate to the first two energy channels (40/90 and 95/230 electron volts). Each succeeding sequence group is delayed by 81.9 seconds as shown in Figure 10.

In Figure 6, we show a few of the bow shock crossings observed during Orbit 1. The first three sequences display a group of interplanetary signals which were typical of the medium at this time. Note the strong roll modulation in channels 4 and 6 (the two highest positive channels) which is centered on the "sun time". This is due to a highly directed flow of protons from the sun. The negative channel (-130/-265 electron volts) displays the usual low-level photocurrent broadly centered around the sun time. After an unfortunate data gap, sequence 1222 shows a highly variable flux of particles which we have interpreted as electrons within the shock transition region. The currents normally observed in these two channels (whenever the satellite is in the magnetosheath) are shown in sequence 1226, some 5.5 minutes later. But even before the eventual entrance into the magnetosheath, the bow shock receded past the satellite and the data indicate interplanetary conditions during sequence 1223.

The last two channels in the M.I.T. format are most interesting. The negative channel indicates interplanetary conditions. The highest positive channel begins as an interplanetary scan at about  $+160^\circ$  with respect to the local sun time. After a graphical foldover of the data to  $-180^\circ$ , the interplanetary conditions persist in the data until roughly  $-45^\circ$ . Then, the

data are seen to rise rapidly from their interplanetary value to a magnitude characteristic of the magnetosheath. The total time lapse for this transition is about one second. If one takes a typical shock velocity of 10 km/sec (Moreno, et al., 1967, Holzer, et al., 1966), then this observation indicates a thin shock of about 10 km thickness. Further support that this was a shock crossing is available from the magnetometer data of Ness and Fairfield (private communication). Their data immediately before our negative channel measurement indicate interplanetary conditions; while 5 seconds after our observed transition, their data show magnetic fields characteristic of the magnetosheath. The plasma data and magnetic field data always show excellent agreement in defining bow shock crossings (Fairfield and Ness, 1967).

Two other bow shock crossings, which are shown in Figures 7 and 8, illustrate measurements which we have interpreted as having been taken within the actual shock layer. The data within sequence 7042 of Figure 7 show the highly variable flux of particles which changes on time scales less than the 3.5 second measurement interval. The character of these data is different from both the interplanetary region (sequence 7038) and the magnetosheath (sequence 7050). The characteristic frequency of the variability (assuming the 0.16 second sampling period introduces negligible aliasing, see Figure 10) is about 1 Hertz which is near the ion cyclotron frequency in this region.

The 260/650 volt channel of sequence 7043 displays a crossing of the shock layer within the frame period. The data begin as characteristic of the magnetosheath at an angle of approximately  $+80^\circ$ . Near  $+180^\circ$  a changeover appears and from  $-180^\circ$  to  $+10^\circ$ , the data display the roll modulation typical of the interplanetary region (see sequence 7039). The satellite next enters the magnetosheath sometime between sequence 7046 and 7047. The slight dip in the negative channel current near the sun time in sequence 7048 is explainable in terms of the out-of-phase photocurrent subtracting from the in-phase electron current.

Another measurement which shows the actual shock boundary crossing is present in Figure 8, sequence 2710. The nearness of the shock layer gives rise to another phenomenon observed here in sequence 2712. Superimposed on an isotropic background current due to refracted electrons, there is a directed flux of protons which is a factor of 20 greater than that normally observed in the interplanetary region (sequences 2704 and 2716). This increase clearly illustrates the presence of particle acceleration mechanisms at or within the shock layer. Prior to the final and complete thermalizing of the streaming plasma, the plasma may undergo several extreme excursions in energy density before reaching the post shock conditions.

A sample of some magnetopause crossings is shown in Figure 9. The three sequences starting with 1322 display the nominal currents observed within the magnetosheath. Sequence 1330 shows the small currents near the instrument's noise level which are

usually seen just inside the magnetosphere. The magnetopause appears to have passed over the satellite during the 700/2000 volt channel of sequence 1331. The data of the next sequence are of the "mixed" variety since they are neither characteristic of the magnetosheath (sequence 1324) nor of the magnetosphere (sequences 1340 and 1344). A magnetopause crossing clearly occurred between the M.I.T. portions of sequence 1339 and 1340. Sequence 1342 shows another "mixed" case, after which the satellite remains in the magnetosphere.

We have investigated in detail the boundary crossings observed during the first twelve orbits of IMP-2. Each crossing was catalogued into one of six types, determined by the character of the signals observed before and after the crossing:

| <u>Type</u> | <u>Description</u>  |
|-------------|---|
| I           | Interplanetary medium/Mixed (IP) (e.g. sequences 1222 and 1223 of Figure 6)     |
| II          | Mixed (IP)/Magnetosheath  |
| III         | Interplanetary medium/Magnetosheath (e.g., sequences 2715 and 2716 of Figure 8) |
| IV          | Magnetosheath/Mixed (MS)  |
| V           | Mixed (MS)/Magnetosphere (e.g., sequences 1342 and 1343 of Figure 9)            |
| VI          | Magnetosheath/Magnetosphere (e.g., sequences 1339 and 1340 of Figure 9)         |

Table II lists the number of crossings within each category, and further subdivides the catalogue into groups determined by the duration of the interval between the observations of the

two signals (Figure 10 depicts the data sampling format).

While there are many statements one can make concerning the data in this table, we wish to call attention to the following general remarks:

a. There are almost twice as many shock crossings as magnetopause crossings, a result which is to be expected due to the lower relative velocity of the satellite near apogee. The number of crossings per unit time is approximately the same for either type. From this we conclude that both boundaries display the same degree of motion and variability.

b. Most of the shock and magnetopause crossings which occurred during the briefest interval of observation (7 seconds) are of the "mixed" type. This suggests that the typical time duration for a boundary traversal is of the order of 5 to 10 seconds. The fact that there are fewer observations of mixed crossings within the long 157-second interval compared to the two 75-second intervals suggests that the mixed crossings are associated with slow, multiple crossings which return in a time period somewhat less than the 157 seconds. Note, however, that the sharp crossings of type III and VI have roughly equal probability of occurrence within the long 157-second interval and the two 75-second intervals, indicating that they are associated with a single, fast crossing.

### 3. Long Period Motion of the Shock Boundary

The previous discussion has concentrated on short-term, generally non-periodic, motion of the boundaries. We wish to

TABLE II

| <u>Type</u>                                    | <u>Within the<br/>two M.I.T<br/>frames<br/>(7 second<br/>interval)</u> | <u>Between<br/>successive<br/>M.I.T. frames<br/>(either of two<br/>75 second<br/>intervals)</u> | <u>Between<br/>formats<br/>(157 second<br/>intervals)</u> | <u>Total</u> |
|--|--|---|---|--------------|
| I  | 20   | 47  | 22  | 89           |
| <u>II</u>                                      | <u>20</u>  | <u>42</u>   | <u>10</u>   | <u>72</u>    |
| Total I & II                                   | 40   | 89  | 32  | 161          |
| III  | 11   | 43  | 53  | 107          |
| Total bow shock crossings (first 12 orbits)    |  |   |   | 268          |
| =====  |  |   |   |              |
| IV   | 5  | 13  | 10  | 28           |
| <u>V</u>                                       | <u>4</u>   | <u>17</u>   | <u>10</u>   | <u>31</u>    |
| Total IV & V                                   | 9  | 30  | 20  | 59           |
| VI   | 1  | 35  | 31  | 67           |
| Total magnetopause crossings (first 12 orbits) |  |   |   | 126          |
| =====  |  |   |   |              |

present here an observation, made during Orbit 15, of an apparent long-period oscillation with a period of 2.7 hours which continued for 12 hours.

The oscillation was apparently triggered by a sudden change in interplanetary conditions which also produced a small sudden commencement at several ground observatories at 1610 hours on 24 October 1964. IMP-2 was outbound on its fifteenth orbit at  $11.6 R_e$ . Shortly after the ssc, the satellite passed briefly into the interplanetary medium at a geocentric distance of  $12.5 R_e$  which was further in than the nominal  $14.2 R_e$  for this region of the dawn hemisphere. Then for some 12 hours the shock boundary passed over the satellite nine times, each crossing being very clearly identifiable (Figure 3) and occurring in a systematic pattern.

We have attempted to model this systematic pattern by a simple sinusoidal motion of the bow shock. Figure 16 presents our results and illustrates that, for this example, the model does quite well in approximating the times of shock crossings. The constant offset of  $14.2 R_e$  applied to the sinusoid is the same as the average value of the shock position in this region. The period of 2.72 hours and the amplitude of  $1.7 R_e$  yield a maximum shock velocity of 7 km/sec.

#### 4. Short Period Motions

Finally, we present some preliminary results of correlations between the M.I.T. plasma data and electrons greater than 45 Kev as measured by the open Geiger tube of the



University of California (Figure 12 and 13). The M.I.T. data are "quantized" into two levels for each figure representing our judgment of the region of space where the satellite is at the time (a "mixed" or uncertain decision is indicated by a dot halfway between the two levels). There are two observations which we would like to mention at this time.

a. The presence of high energy electron spikes near the shock is associated with the multiplicity of bow shock crossings. After the satellite finally passed into the magnetosheath (indicated by T on Figure 12), the counting rate of these electrons dropped to background levels.

b. The presence of high energy electron spikes near the magnetopause is associated with the occasional passage of the satellite into and out of the magnetosphere. There is a one-to-one relationship between spikes and an excursion into the magnetosphere. Once the outer region of the magnetosphere has been entered, the counting rate continues to rise although it still shows the effects of boundary motion.

### III. Summary

The data from the M.I.T. plasma experiment on IMP-2 have shown that the boundaries of the magnetosheath are extremely pliable and responsive to solar and geomagnetic activity. Further, even during relatively quiet periods, the boundaries appear to remain in motion although on a smaller scale. Both long term (hours) and short term (minutes) periodicities have been observed. The actual shock boundary layer has been observed, and rapidly varying fluxes in energy and direction are characteristic of the layer.

## ACKNOWLEDGEMENTS

The author is grateful for the many helpful discussions with Dr. H. S. Bridge and Dr. V. Vasylunas of M.I.T. The communications and exchange of data with D. Fairfield of GSFC, and K. A. Anderson of the University of California are greatly appreciated.

This research has been supported in part by the National Aeronautics and Space Administration under contract NAS-5-2952 and grant NsG-386, and in part by the Atomic Energy Commission under contract At(30-1)-2098.

## REFERENCES

- Anderson, K. A., Private Communication, University of California, Berkeley, 1967.
- Binsack, J. H., Plasmopause Observations with the MIT experiment on IMP-2, to be published in J. Geophys. Res., 1967.
- Binsack, J. H. and V. Vasylunas, Simultaneous IMP-2 and OGO-1 Observations of Bow Shock Compression, submitted to J. Geophys. Res., 1967.
- Fairfield, D. H., Private Communication, Goddard Space Flight Center, Greenbelt, Maryland, 1966.
- Fairfield, D. H. and N. Ness, Magnetic Field Measurements with the IMP-2 Satellite, J. Geophys. Res., 72, 2379-2403, May 1, 1967.
- Holzer, R. E., M. G. McLeod and E. J. Smith, Preliminary Results from the OGO-1 Search Coil Magnetometer: Boundary Positions and Magnetic Noise Spectra, J. Geophys. Res., 71, 1481-1486, 1966.
- Moreno, G., S. Olbert, G. L. Pai, and A. Egidi, Final Results of the MIT Plasma Experiment on IMP-1, II. The Transition Region, submitted to the J. Geophys. Res., 1967.

## FIGURE CAPTIONS

Figure 1—General Schematic of the M.I.T. Plasma Detector

Figure 2—The region of space explored by IMP-2 during its three "lifetimes". The projection is onto the solar ecliptic XY plane. The average locations of the shock and magnetopause boundaries are taken from IMP-1 (Moreno, et al., 1967).

Figure 3—Summary plot of Orbit 15. For each 5.45 minute interval, two quantities are plotted for each channel: the maximum current for each channel observed during the spin period, and the average current observed in a  $60^\circ$  segment centered in the antisolar direction (only the latter is plotted for the negative channel). See text for discussion.

Figure 4—The portions of the IMP-2 orbits where plasma characteristic of the magnetosheath (transition region) were observed. The plane of presentation is defined by the sun-earth and earth-satellite lines. The small circles at the end of a trace indicate the position of the first or last observation of the bow shock for that orbit (some orbit numbers are included where convenient). Arrows indicate missing data beyond that point.

Figure 5—Detailed space-time positions of the observations of plasma characteristic of the magnetosheath during the first seven orbits. There were geomagnetic storms prior to Orbit 1 and prior to the inbound portion of Orbit 6.

Figure 6—Bow Shock Crossing, Orbit 1. Detailed plots of the data within each energy channel. For each channel the data is displayed on an axis from  $-180^\circ$  to  $0^\circ$  to  $+180^\circ$ , where zero degrees corresponds to the time when the detector was closest to the satellite-sun line. The starting time of the individual channel may be anywhere with respect to the zero degree marker; we have therefore folded over the data if it exceeded  $+180^\circ$ . See Figure 10 for the time sequencing of the data samples.

Figure 7—Bow shock crossing, Orbit 5 (see Figure 6).

Figure 8—Bow shock crossing, Orbit 2 (see Figure 6).

Figure 9—Magnetopause crossing, Orbit 1 (see Figure 6).

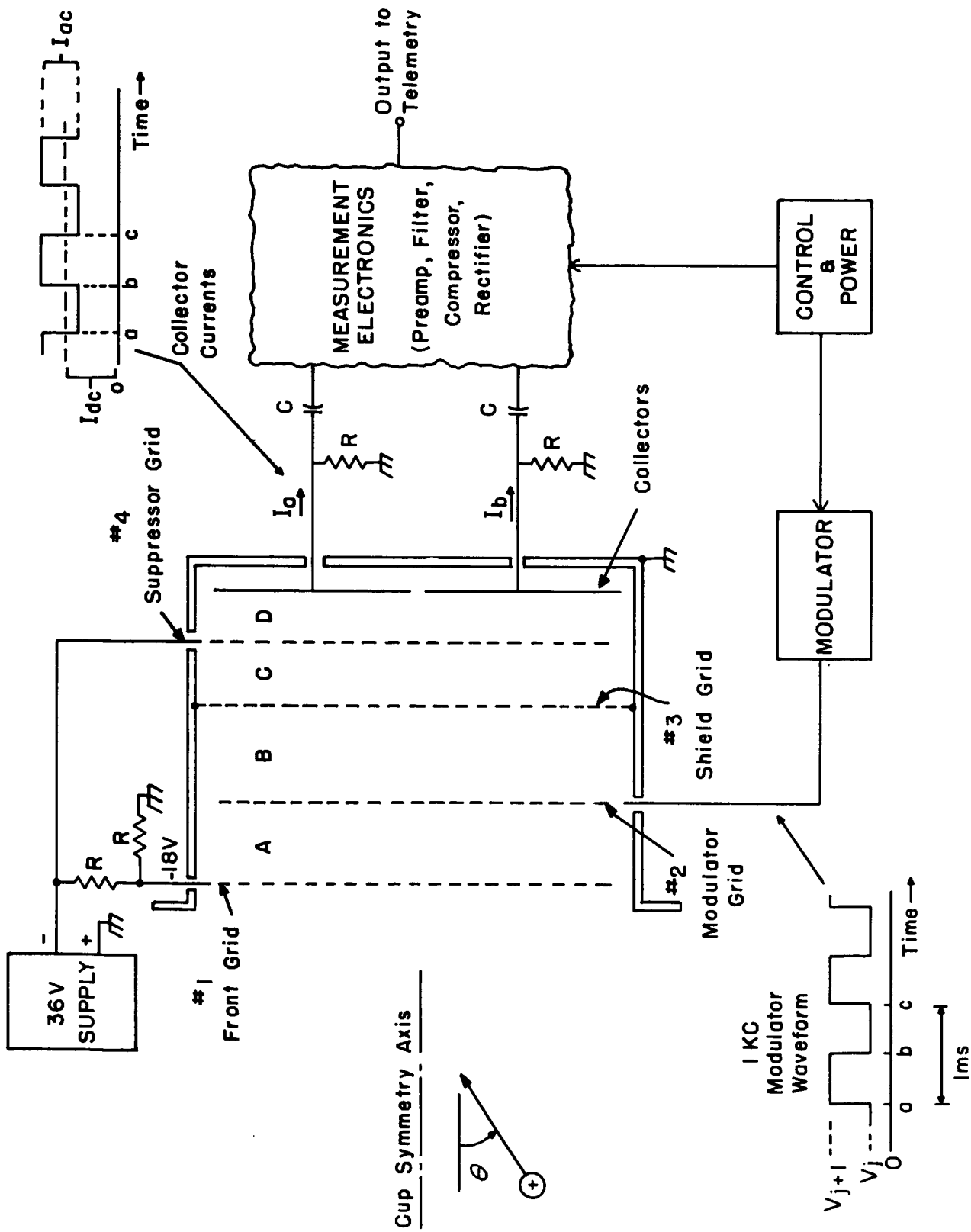
Figure 10—The time sequencing of the M.I.T. experiment on IMP-2. The basic telemetry format is composed of 4 sequences: the first three are time multiplexed among the experimenters, the fourth is completely devoted to the Rb Vapor magnetometer. Within each of the three data sequences, frames 13 and 14 are used by the M.I.T. experiment. In sequences of type 1 frame 13 monitors the plasma in the 40/90 eV energy range, and frame 14 in the 95/230 eV range. Frames 13 and 14 of sequences of type 2 monitor the energy ranges 260/650 and 700/2000 eV respectively. Frames 13 and 14 of sequences of type 3 monitor the energy range -130/-265 and 1800/5400 respectively.

Within each frame there were 22 useful samples of the plasma taken over 3.52 seconds (which was usually shorter than a complete spin period).

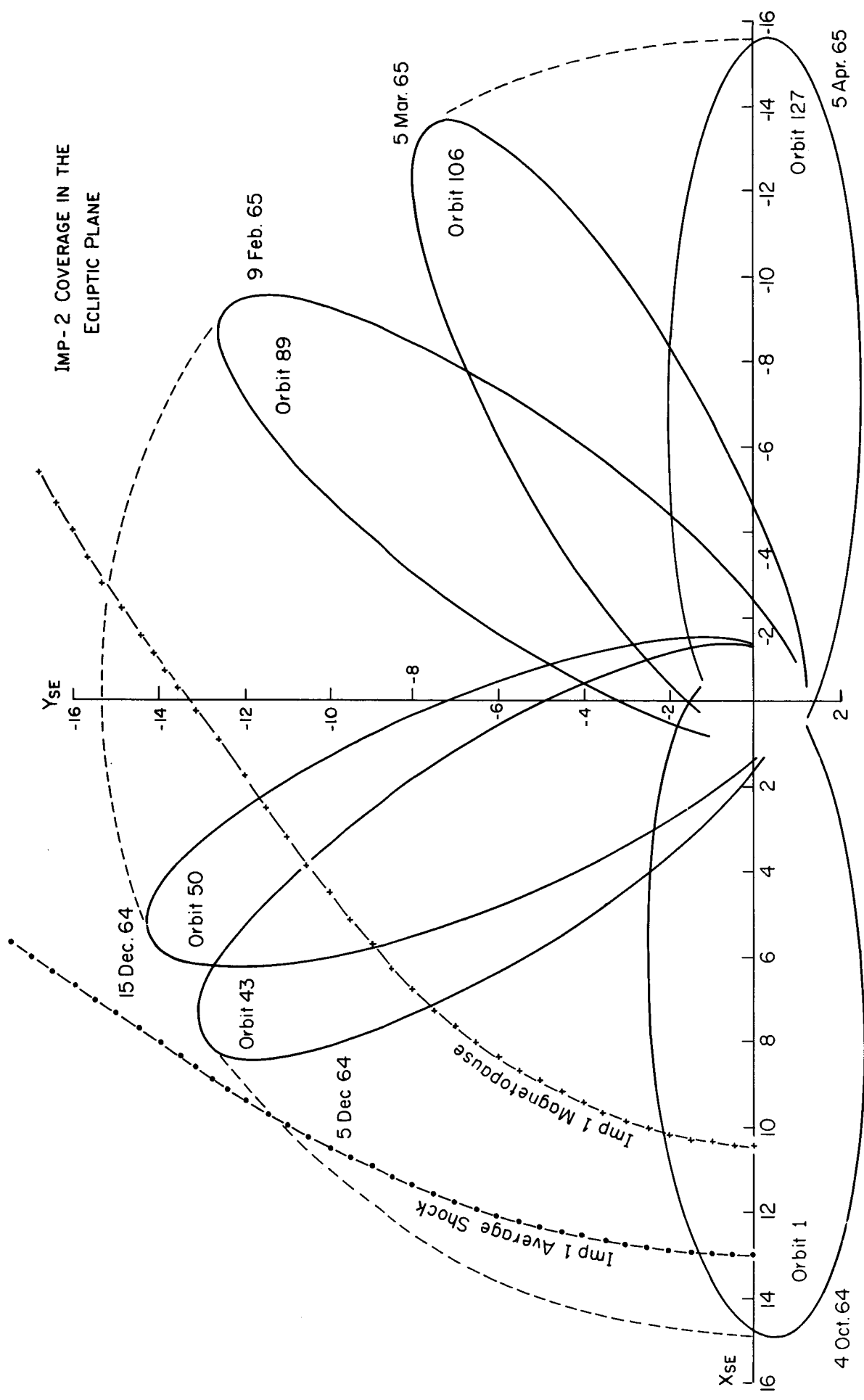
Figure 11—A model long period shock oscillation for the observations during Orbit 15. The amplitude of 1.7 Re and period of 2.72 hours yield a maximum shock speed of 7 km/sec at the nominal quiet time shock location of 14.2 Re.

Figure 12—Comparison of the University of California Geiger Tube (electrons > 45 Kev) counting rate and the M.I.T. plasma data. The plasma data are used to determine if the satellite was in the interplanetary region (I.P.), the magnetosheath (T) or the magnetosphere (M).

Figure 13—(See Figure 12).



IMP CUP





STANDARD FORM NO. ONE HUNDRED

IMP-B QBBIT NQ. 15 24-25 OCT. 1964

-1351-265

ANGLE OF MEY.

1800/5400

701928

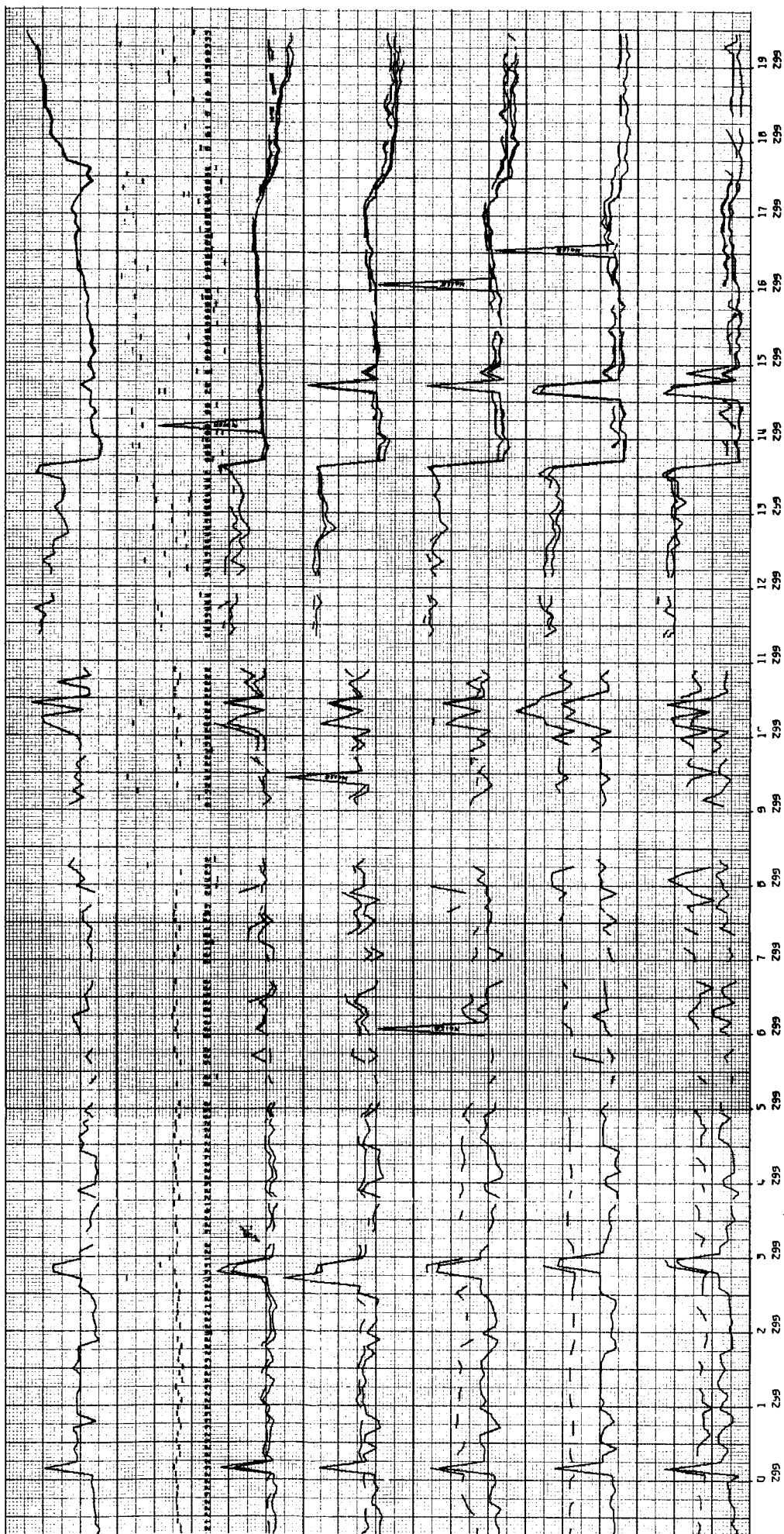
05J109Z

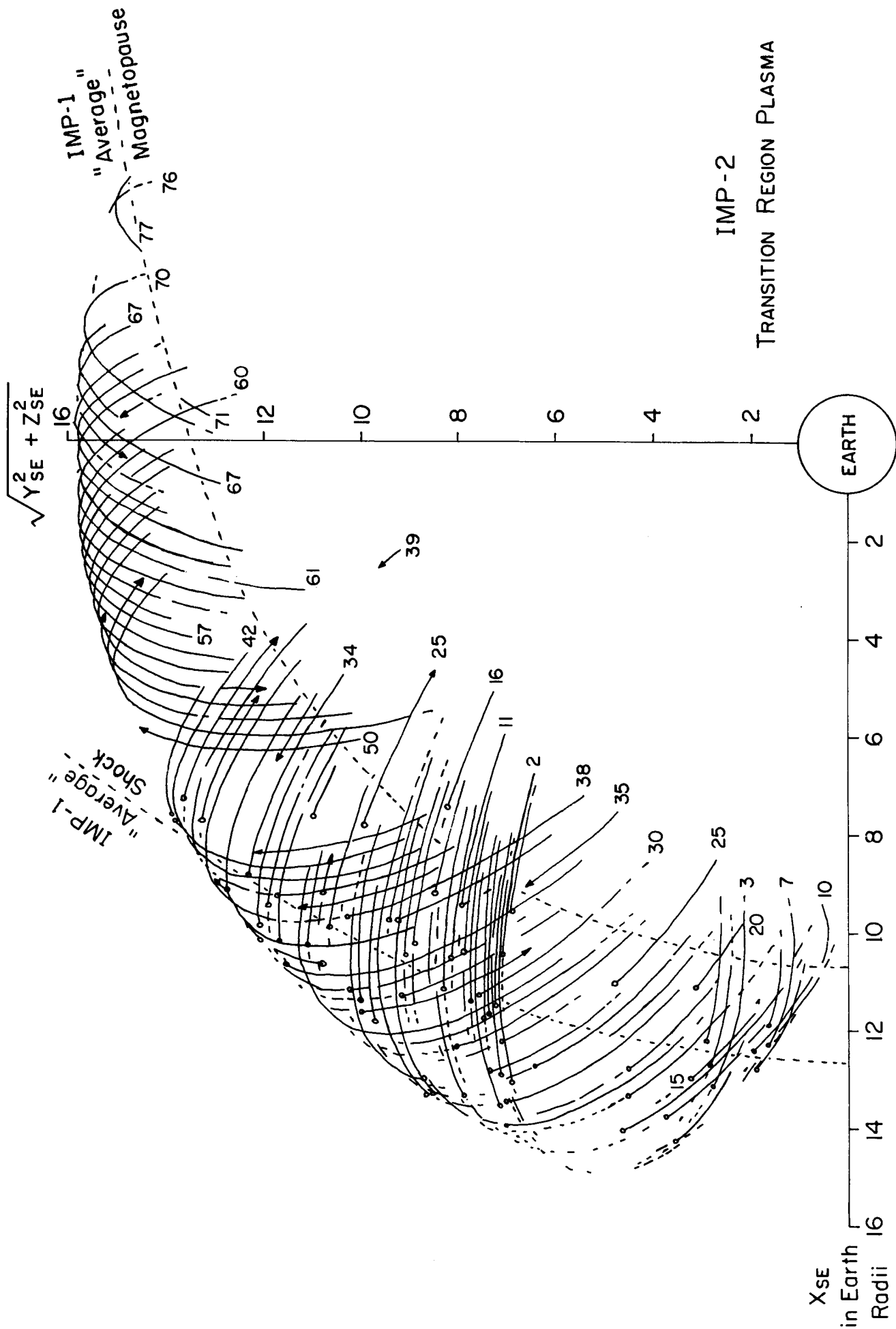
954230

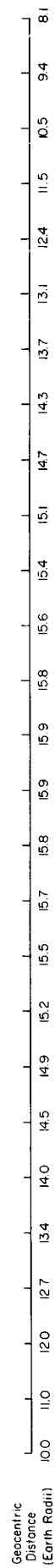
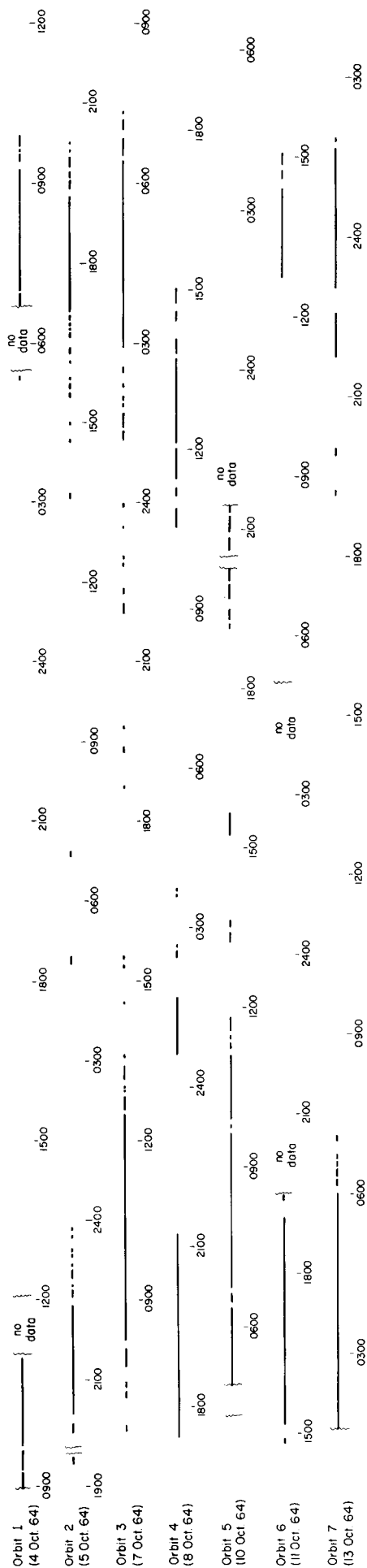
06/05/11

Page 100

RSO I RSO



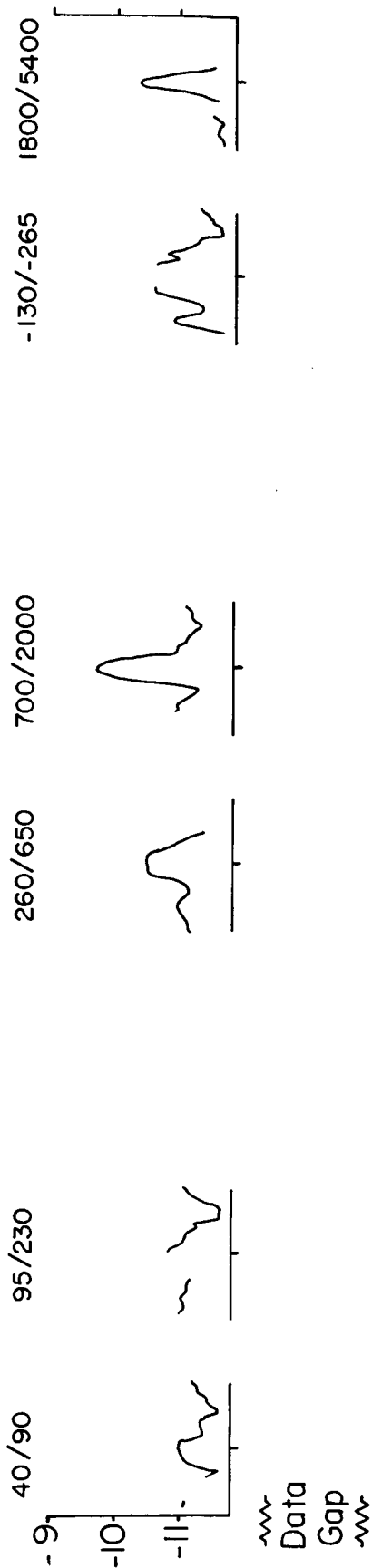




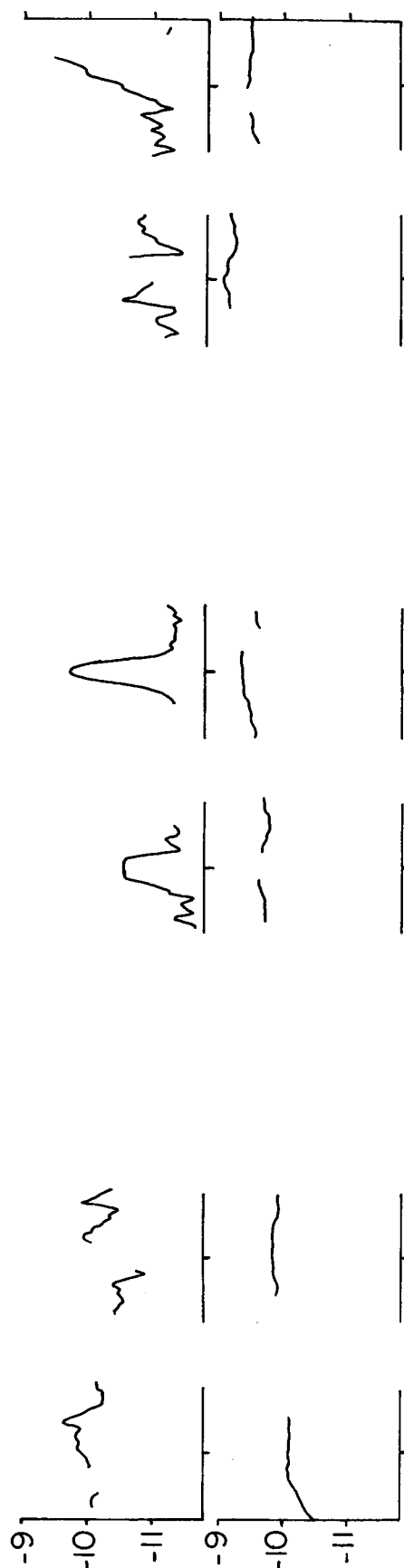
DETAILED SPACE-TIME POSITIONS OF TRANSITION-LIKE PLASMA FOR  
IMP-2 ORBITS 1-7

M.I.T. IMP-2  
LOG CURRENTS IN INDIVIDUAL ENERGY CHANNELS

Seq. no. 1158  
Time 0526  
Oct. 5

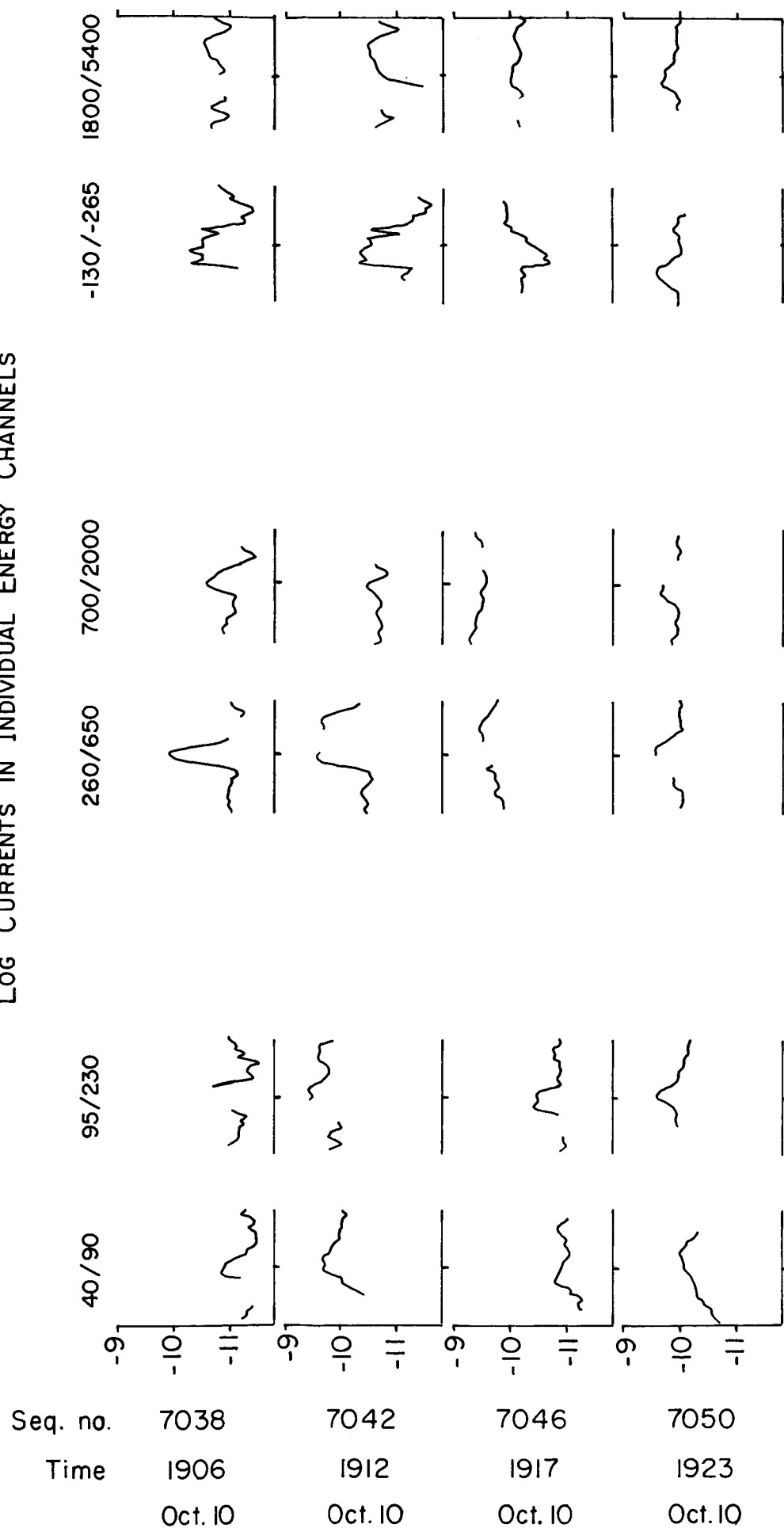


1222 1226  
0653 0658  
Oct. 5 Oct. 5



Bow Shock Crossings, Orbit 1 Inbound

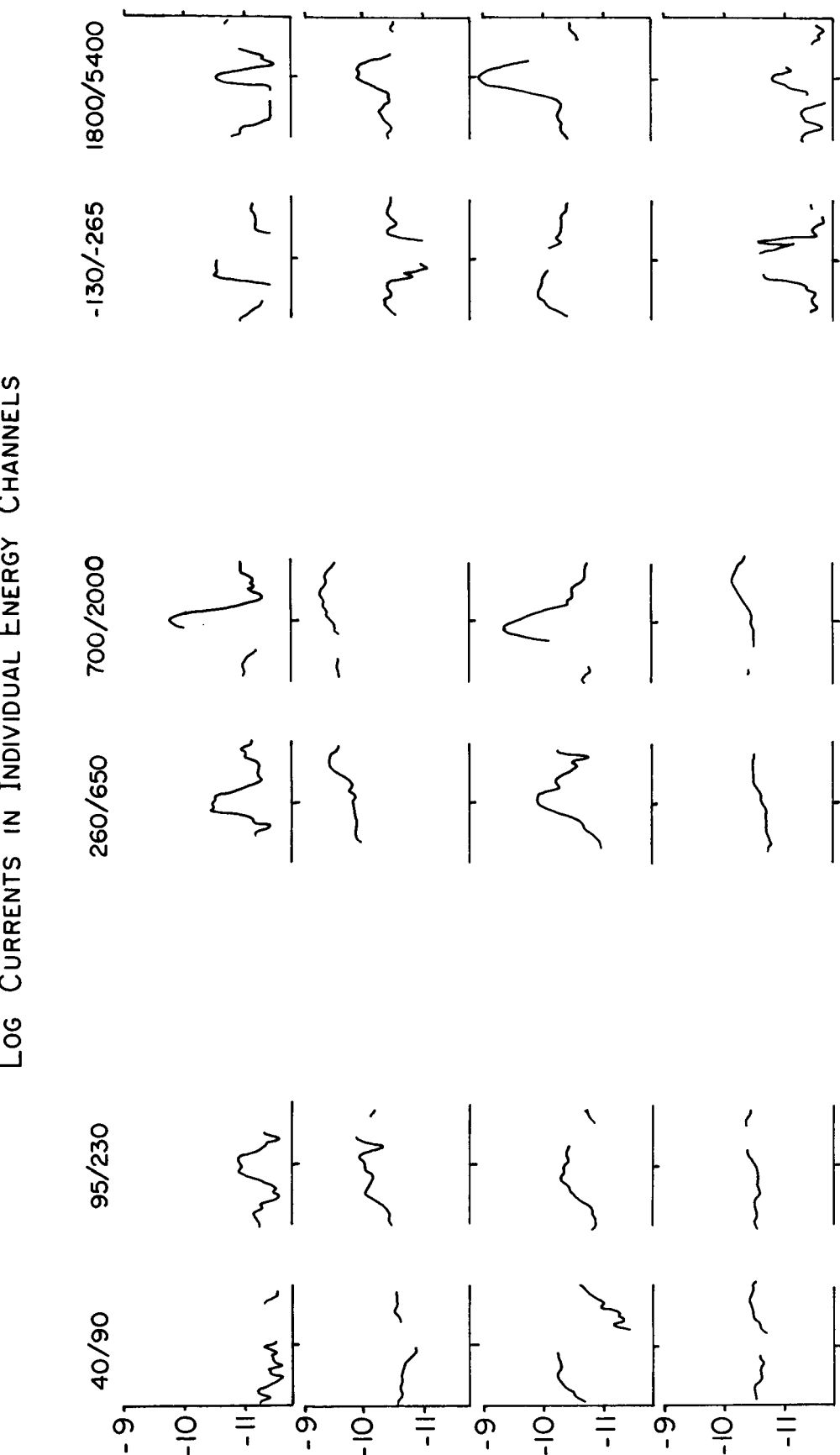
M.I.T. IMP-2  
LOG CURRENTS IN INDIVIDUAL ENERGY CHANNELS



Bow Shock Crossings, Orbit 5 Inbound

# M.I.T. IMP -2

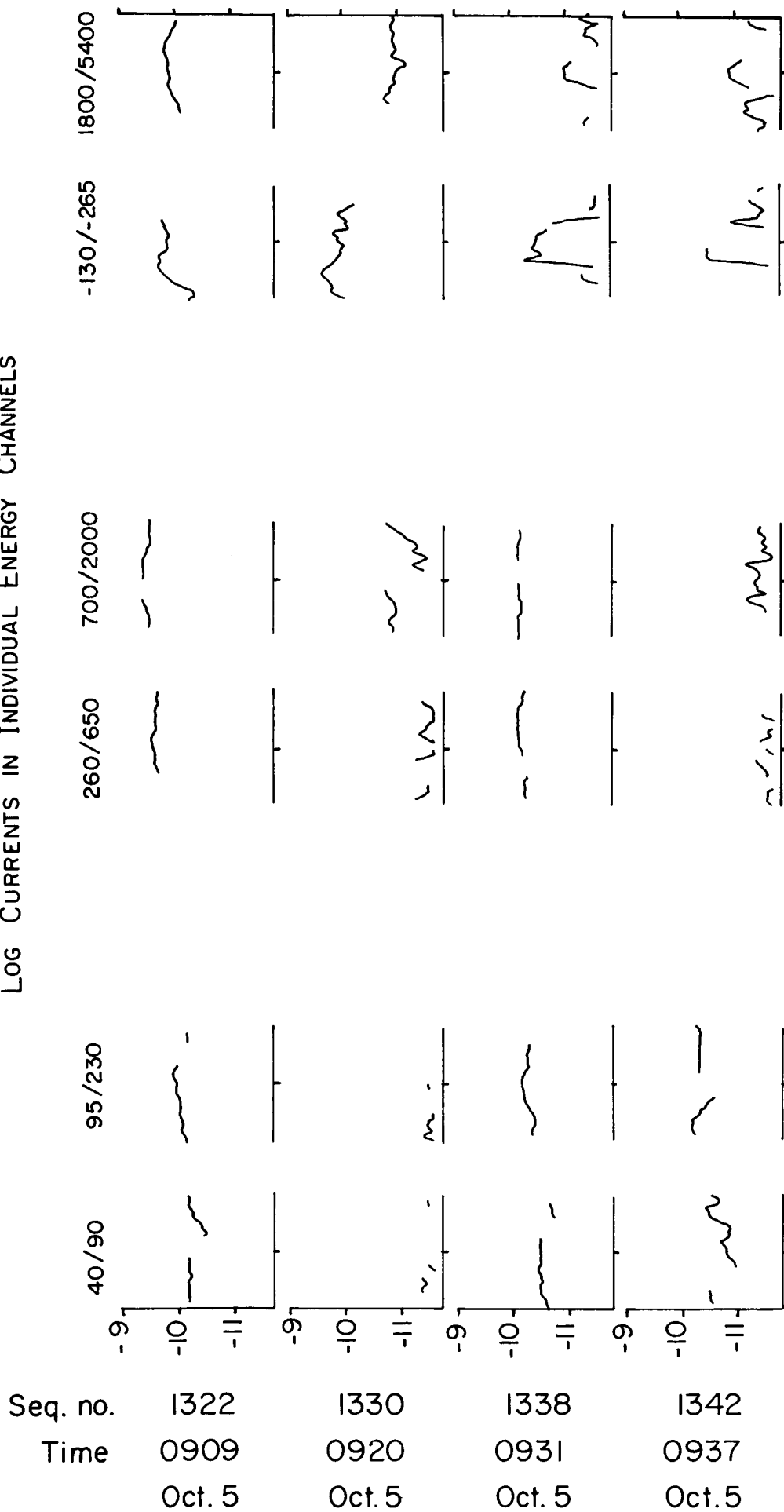
## LOG CURRENTS IN INDIVIDUAL ENERGY CHANNELS



| Seq. no. | 2702   | 2706   | 2710   | 2714   |
|----------|--------|--------|--------|--------|
| Time     | 1632   | 1637   | 1643   | 1648   |
|          | Oct. 6 | Oct. 6 | Oct. 6 | Oct. 6 |

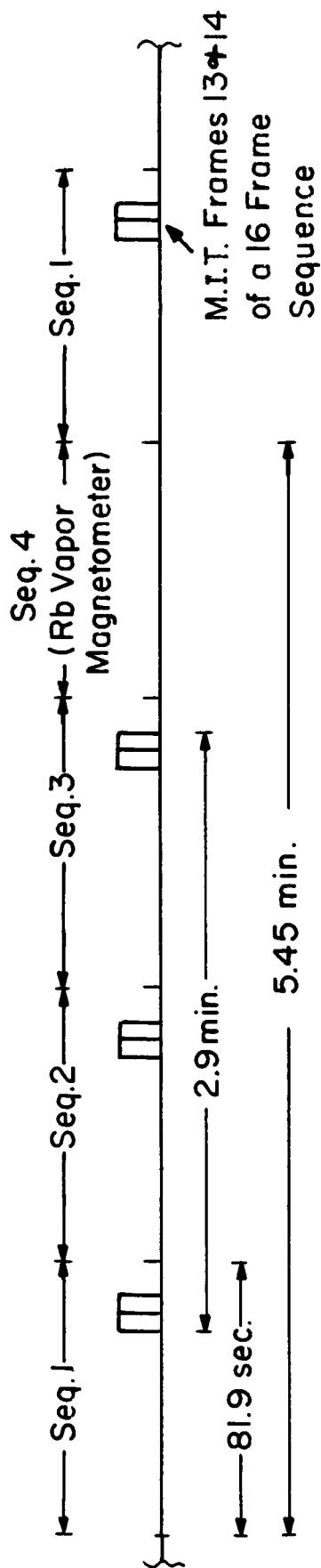
Bow Shock Crossings, Orbit 2 Inbound

M.I.T. IMP-2  
LOG CURRENTS IN INDIVIDUAL ENERGY CHANNELS

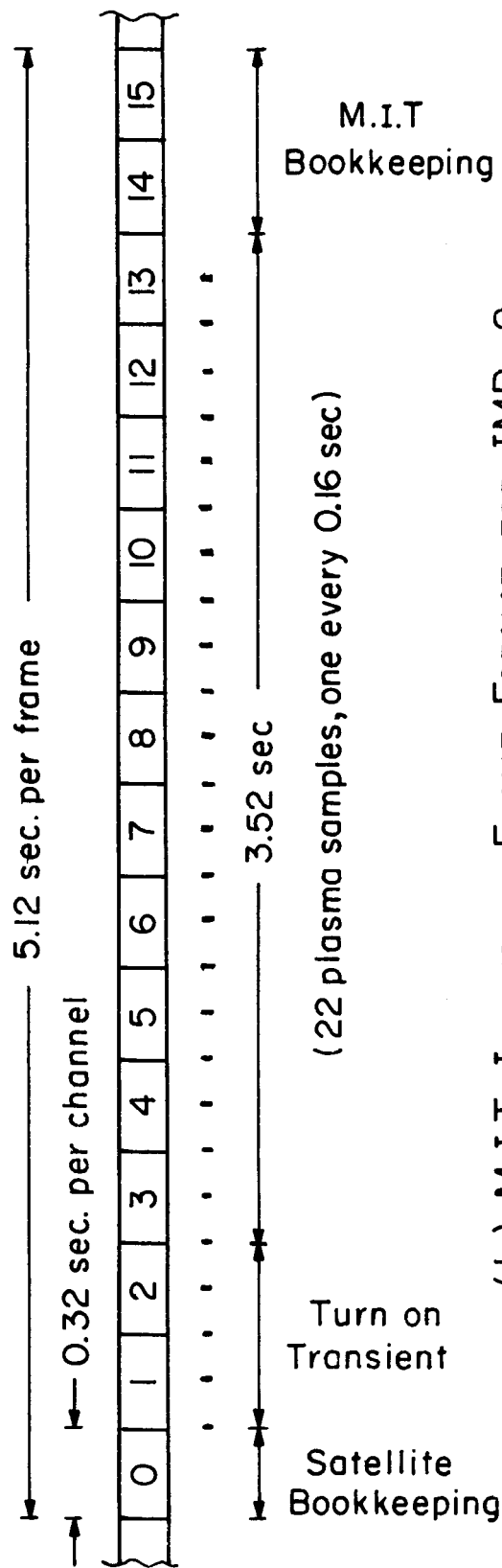


Magnetopause Crossings , Orbit 1 Inbound

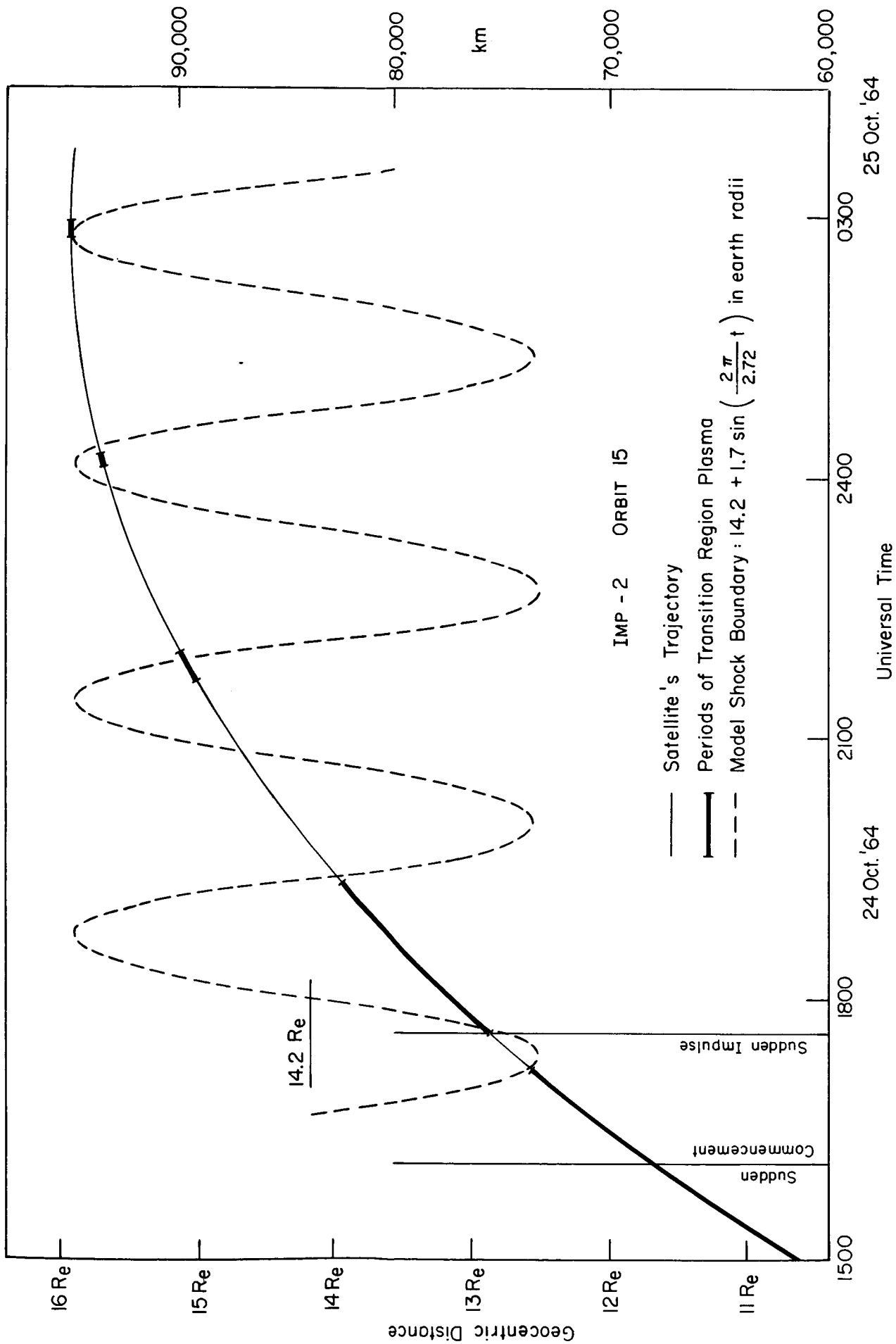




(a) M.I.T. DATA FRAMES WITHIN THE IMP - 2 FORMAT

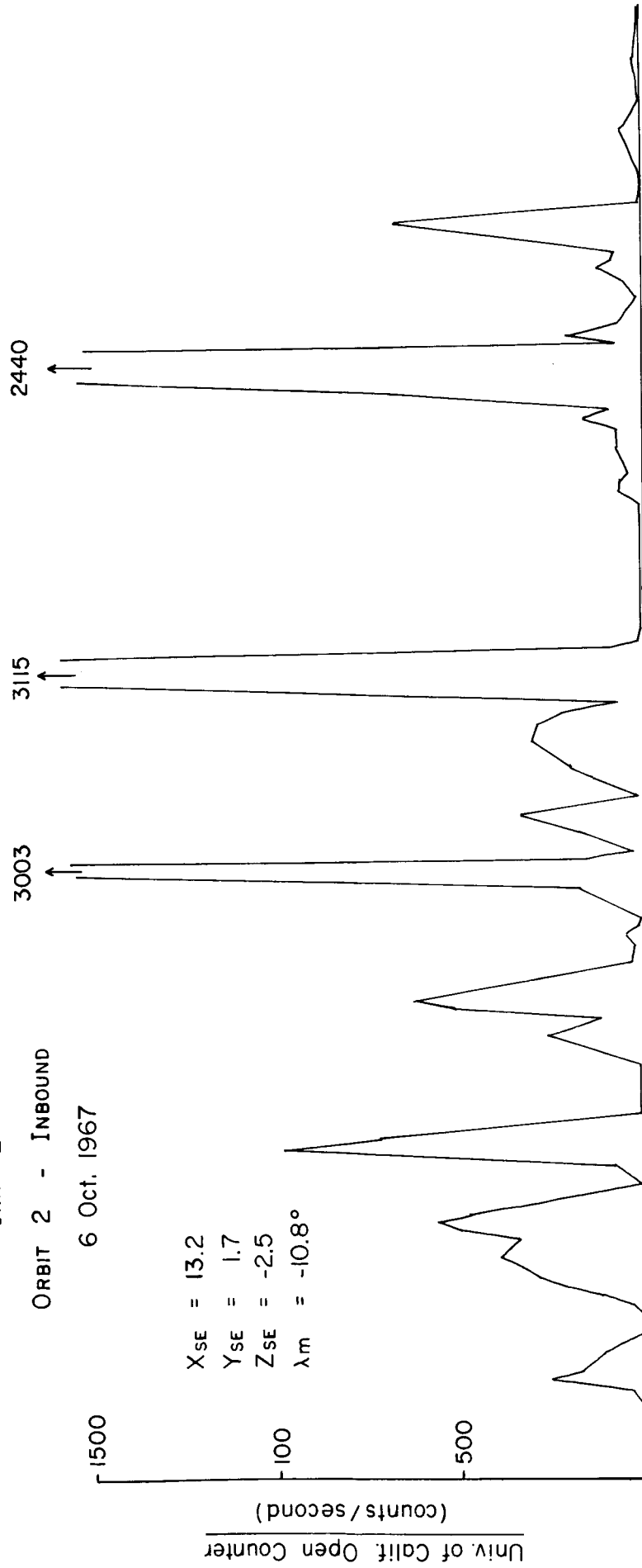


(b) M.I.T. INDIVIDUAL FRAME FORMAT FOR IMP - 2



IMP - 2  
ORBIT 2 - INBOUND  
6 Oct. 1967

$X_{SE} = 13.2$   
 $Y_{SE} = 1.7$   
 $Z_{SE} = -2.5$   
 $\lambda_m = -10.8^\circ$



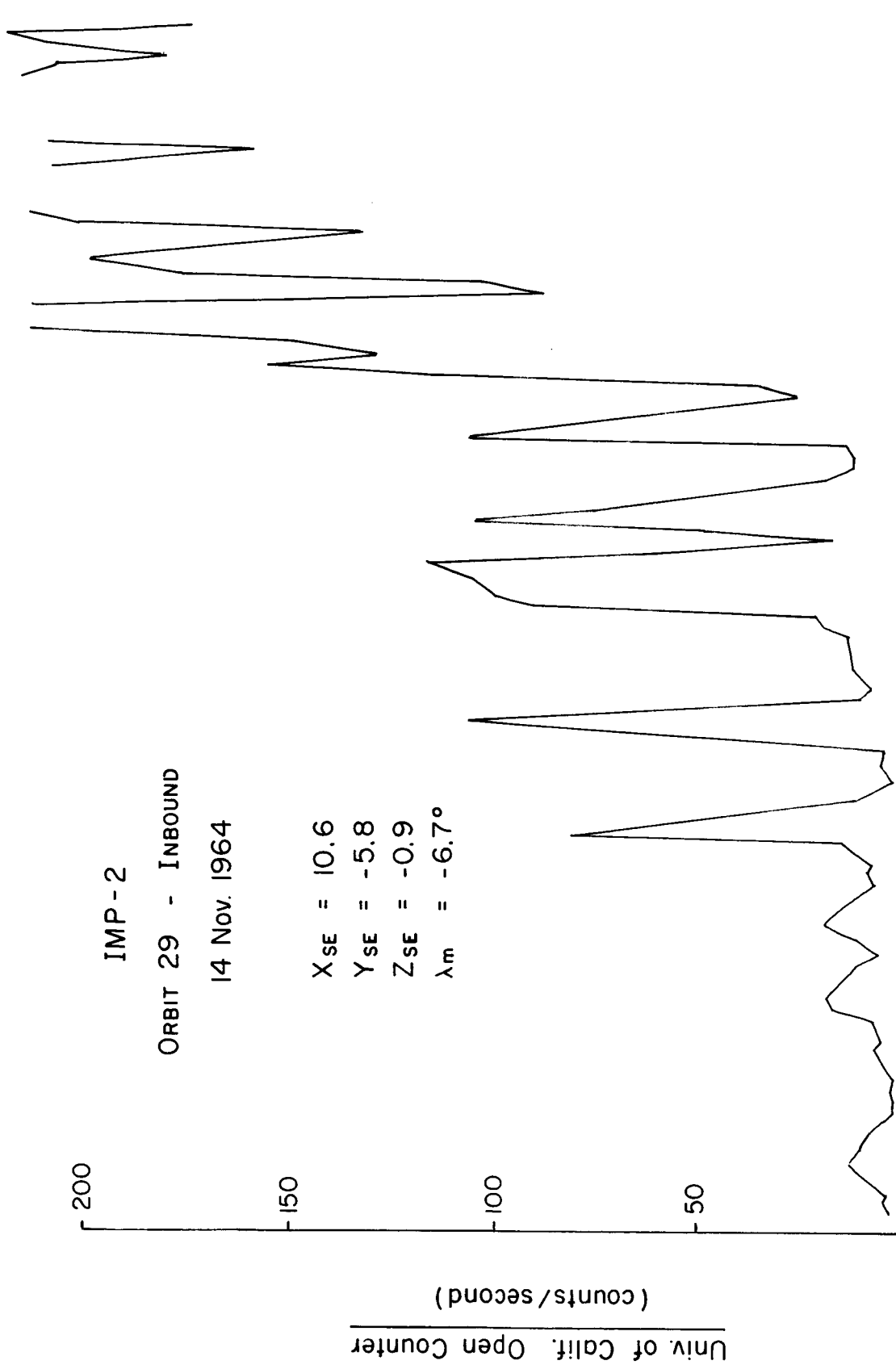
M.I.T. Plasma

I.P. → . . . .

T → . . . .

Seq. No.

Time (U.T.) 1530 1540 1550 1600 1610 1620 1630 1640 1650 1660 1670 1680 1690 1700 1710



M.I.T. Plasma

M →

T →

| Seq. No. | Time (U.T.) |
|----------|-------------|
| 43900    | 1710        |
| 43910    | 1720        |
| 43920    | 1730        |
| 43930    | 1740        |
| 43940    | 1750        |
| 43950    | 1800        |
| 43960    | 1810        |
|          | 1820        |
|          | 1830        |